Hindawi
Advances in Materials Science and Engineering
Volume 2018, Article ID 1653484, 9 pages
https://doi.org/10.1155/2018/1653484

Research Article

Organic Phosphorus Compounds as Inhibitors of Corrosion of Carbon Steel in Circulating Cooling Water: Weight Loss Method and Thermodynamic and Quantum Chemical Studies

Liang Liu, Ting-Ting Cao, Qi-Wei Zhang, and Chong-Wei Cui

Harbin Institute of Technology, School of Environment, Harbin 150090, China

Correspondence should be addressed to Chong-Wei Cui; cuichongwei1991@126.com

Received 14 August 2018; Revised 28 October 2018; Accepted 7 November 2018; Published 2 December 2018

Academic Editor: Alfredo Juan

Circulating cooling water plays an important role in industrial water use. In this study, the corrosion inhibition effects of PBTCA, HEDP, and ATMP organic phosphorus inhibitors were investigated using the weight loss method by varying the dosage of inhibitors, ClO_2 concentrations, and pH values on carbon steel in recirculating cooling water with a low concentration of ClO_2 solution. The results showed that the three corrosion inhibitors had a satisfactory corrosion inhibition effect and that corrosion inhibition efficiency is positively correlated with the concentration of organic phosphorus inhibitors and pH. The average corrosion inhibition efficiency of the three inhibitors was about 80% at the concentration of inhibitors = 35 mg/L, pH = 9.0, and the concentration of ClO_2 = 7.0 mg/L, of which the single-phosphorus molecular corrosion inhibitor proved to be the best inhibitor. When the ClO_2 concentration was 7 mg/L, the corrosion inhibition efficiencies of the three corrosion inhibitors were relatively stable. Using the density functional theory (DFT) algorithm in the Gaussian 09 program, the optimization calculation was completed by the B3LYP/6-31G (d, p) method at the microlevel. The molecular structures of the three organic phosphorus inhibitors and the number of phosphorus-containing atoms were compared to the sustained-release properties. Organic phosphorus inhibitors, as an electronic buffer, not only provided electrons but also received electrons. They formed a complex with iron and zinc ions in water in order to attach to the surface of the carbon steel and to alleviate corrosion. In addition, the adsorption with a metal surface followed the Langmuir adsorption isotherm.

1. Introduction

Circulating cooling water accounts for 60–90% of total industrial water use [1–3]. Because of continuous recycling, the water quality of circulating cooling water becomes more concentrated leading to corrosion, fouling, and microbial breeding [4–6], which results in lower heat transfer efficiency of heat exchangers, corrosion and perforation of metal pipelines, and safety issues [7, 8].

Since the 1930s, the use of organic phosphorus inhibitors in circulating cooling water has alleviated the corrosion of carbon steel [9, 10]. To inhibit microbial breeding in circulating cooling water, oxidizing or nonoxidizing fungicides are added to the water [9, 11, 12]. The combined use of the corrosion inhibitor and the bactericide has relieved the impact of the challenges mentioned above and has promoted the development of the industrial economy. Organic phosphorus inhibitors, and also in combination with ClO_2, have good corrosion inhibition properties, but there are only a few articles about their corrosion inhibition mechanism with carbon steel [13, 14]. A large number of studies have shown that the efficiency of corrosion inhibitors is closely related to their structures [15–17]. The quantum chemical method can be used to calculate the molecular structure parameters and to explore the mechanism of corrosion inhibition at the microlevel [18, 19]. Kumar et al. [20] used the AM1 semiempirical quantum chemical method to study the corrosion inhibition mechanism of synthetic organic matter for N80 carbon steel and found that the adsorption of inhibitors followed the Langmuir adsorption isotherm. Gece and Bilgi [21] used the B3LYP/6-311 ++ G (d, p) method to study the mechanism of a nitrogen corrosion inhibitor in

acidic media and concluded that the nitrogen atom belongs to the active centre and has good corrosion inhibition performance. Shi et al. [22] studied the adsorption behaviour of four pyrazine inhibitors on a copper surface using the density functional theory and the difference in charge density and distribution analysis. The vertical adsorption of the corrosion inhibitor molecules on the metal surface was by chemical adsorption where the coordination bond was formed. By analyzing the frontier orbitals, it was verified that the active site of the inhibitor was the N atom on the pyrazine ring.

Hitherto, good results have been obtained in the research of nitrogen corrosion inhibitors, but few reports have described the mechanism of action between phosphorus corrosion inhibitors and metal surfaces. In this paper, three kinds of organic phosphorus corrosion inhibitors: 2-phosphate group-1,2,4-tricarboxylate butane (PBTCA), hydroxyethylidene disphosphonic acid (HEDP), and aminotrimethylene phosphonic acid (ATMP), were studied. The corrosion inhibition performance of the organophosphorus corrosion inhibitors in combination with ClO_2 on the carbon steel was analyzed experimentally. The charge distribution, frontier orbit, and adsorption model of stable molecules were investigated using ChemBioOffice 2014, Gaussian 09, and Origin 2017 software to explore the corrosion inhibition mechanism of the organic phosphorus inhibitor on the metal surface and provide theoretical support for its application in circulating cooling water.

2. Experimental Materials and Research Methods

2.1. Experimental Material. The composition and content of the standard water used in the experiment are shown in Table 1.

2.2. Weight Loss Method. The effect of different inhibitor concentrations, ClO_2 concentrations, and pH values on the corrosion inhibition efficiency of the corrosion inhibitors on carbon steel in circulating cooling water with a low concentration of ClO_2 and zinc ion solution was studied by using the weight loss method. Determination methods and procedures were referenced to the regulation of corrosion resistance of water treatment agents (GB/t 18175-2014) [23, 24]. The corrosion rate V and corrosion inhibition efficiency E were determined using the following equations:

$$V = K\frac{W1 - W2}{F \times t \times \gamma},$$
$$E = \frac{C_0 - C_t}{C_0} \times 100, \quad (1)$$

where $W1$ and $W2$ are the weight of specimens before and after corrosion, respectively; F is the surface area of the specimen exposed to cooling water; K is a constant, whose value is 87.6; t is the specimen immersion corrosion time; γ is the metal density; and C_0 and C_t are corrosion rates in the absence and presence of the inhibitor, respectively.

Table 1: The composition and content of the standard water used in the experiment.

Ion	Ca^{2+}	Mg^{2+}	Na^{+}	Zn^{2+}	Cl^{-}	SO_4^{2-}	HCO_3^{-}
Concentration (mg/L)	200	48	305	5	426	192	122

2.3. Quantum Chemical Calculation. The molecular structures of organic phosphorus inhibitors PBTCA, HEDP, and ATMP were constructed using ChemBioDraw Ultra 14.0, and the RHF/6-31G method of GAMESS was used to preliminarily optimize the structure. Density functional theory (DFT) helps to study the electronic structure of a multielectron system with high computational accuracy [25], so the DFT algorithm in the Gaussian 09 program was used, without any symmetry restriction being imposed, in the B3LYP/6-31G (d, p) method [26]. The quantum chemical parameters and related parameters of each molecule were obtained from the output results by optimizing the three inhibitors. The stable composition of the three corrosion inhibitors after optimization is shown in Figure 1. The quantum chemical parameters included the highest occupied molecular orbital energy (E_{HOMO}), the lowest unoccupied molecular orbital energy E_{LUMO}, the energy gap (ΔE), the distribution of the atomic Mulliken charge, and the molecular dipole moment (μ). Other relevant parameters included the ionization potential (I), electronegativity χ, electron affinity (A), hardness (η), and affinity index (ω). These parameters were calculated using the following equations [27]:

$$I = -E_{HOMO},$$
$$A = -E_{LUMO},$$
$$\chi = \frac{I + A}{2},$$
$$\eta = \frac{I - A}{2},$$
$$\omega = \frac{\chi^2}{2\eta}. \quad (3)$$

3. Results and Discussion

3.1. Evaluation of Corrosion Inhibition Performance of Organophosphorus Agents. PBTCA, HEDP, and ATMP are commonly used water treatment agents, and they have excellent corrosion and scale inhibition and a moderate price and are suitable for large-scale use. In this section, we studied the influence of three factors: corrosion inhibitor concentration, ClO_2 concentration, and pH value, on the corrosion inhibition efficiency of corrosion of carbon steel.

3.1.1. Effect of Inhibitor Concentration on the Inhibition of Corrosion of Carbon Steel. The effect of the concentration of PBTCA, HEDP, and ATMP on the inhibition of corrosion of

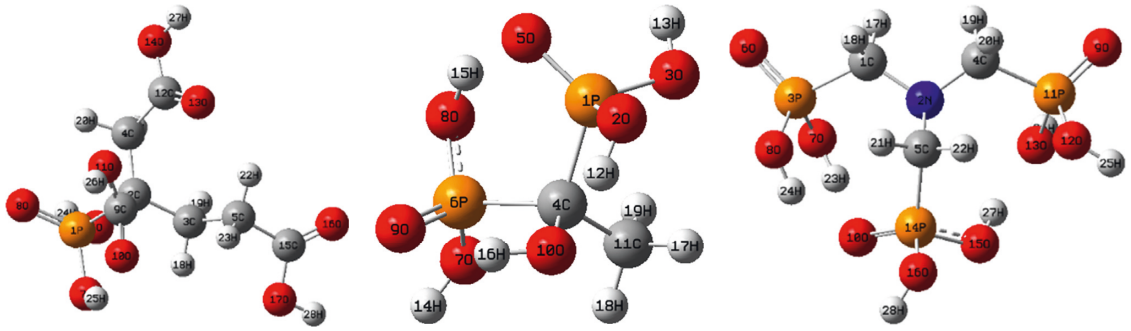

(a) (b) (c)

Figure 1: Molecular model diagram of three organophosphorus inhibitors. (a) PBTCA. (b) HEDP. (c) ATMP.

carbon steel was studied using the carbon steel test, and the test liquid was a mixture of standard water, ClO_2, and corrosion inhibitor. The concentration of ClO_2 was 7.0 mg/L, the temperature was (40.0 ± 1.0)°C, the pH was 9.0, and the rotation reaction time was 72 h. The experiment was repeated three times, and the average values are shown in Figure 2.

The above figure shows that, with the increasing organic phosphorus concentration, the inhibition rate increased gradually and the average inhibition rate of the three corrosion inhibitors reached above 80%. When the concentration was increased to 35.0 mg/L, the corrosion inhibition rate of ATMP was more than 70%. Figure 2 shows that the corrosion inhibition rate of three corrosion inhibitors is in the order of PBTCA > HEDP > ATMP based on the number of phosphorus atoms in the inhibitor. The results also show that the inhibition performance is related to the number of P atoms, and the single-phosphorus molecule inhibitor exhibits a preferable corrosion inhibition effect.

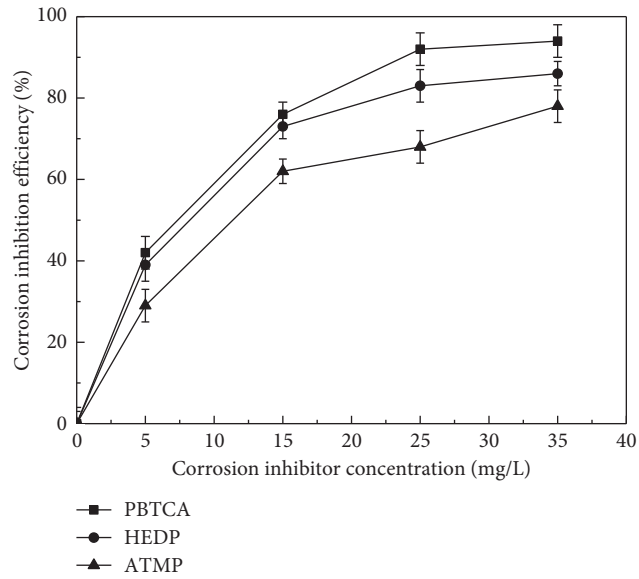

Figure 2: Effect of concentration of the three corrosion inhibitors on the inhibition of corrosion of carbon steel.

3.1.2. Effect of ClO_2 Concentration on Corrosion Inhibition of Carbon Steel. ClO_2 is a good fungicide and can be combined with a corrosion inhibitor by the compounding technology. The test solution was a mixture of standard water, ClO_2, and corrosion inhibitor. The effect of the ClO_2 concentration on the inhibition of corrosion of carbon steel was studied. The corrosion inhibitor concentration was 15.0 mg/L, the temperature was (40.0 ± 1.0)°C, the pH was 9.0, and the rotation reaction time was 72 h. The experiment was repeated three times, and the average results are shown in Figure 3.

From Figure 3(a), it can be seen that the addition of ClO_2 had a certain inhibitory effect on the slow-release performance of the three inhibitors, but the compound of an inhibitor and ClO_2 still had good corrosion inhibition effect. When the ClO_2 concentration was increased, the slow-release performance of HEDP steadily decreased. Generally, the average slow-release performance of HEDP and ATMP was lower than that of PBTCA. The slow-release performance of PBTCA showed fewer fluctuations, and its slow-release performance was more stable with ClO_2 concentration changes as compared with the inhibitors HEDP and ATMP (Figure 3(b)). However, with the increase in ClO_2 concentration, the inhibition rate of ATMP decreased, and the lowest inhibition rate recorded was only about 30%.

Once the concentration of ClO_2 was 7 mg/l, the slow-release performance of PBTCA and HEDP was significantly higher than that of ATMP. Overall, the average corrosion inhibition rate of the three corrosion inhibitors in the presence of ClO_2 was PBTCA > HEDP > ATMP.

3.1.3. Effect of pH on Inhibition of Corrosion of Carbon Steel. The test solution in this test was a mixture of standard water, ClO_2, and corrosion inhibitor, and the effect of pH on corrosion inhibition was determined. The initial concentration of the corrosion inhibitor was 15.0 mg/L, the ClO_2 concentration was 7.0 mg/L, the temperature was (40.0 ± 1.0)°C, and the rotation reaction time was 72 h. The experiment was repeated three times, and the average results are shown in Figure 4.

The inhibition rate of the three organic phosphorus reagents increased with increasing pH, indicating that the protective film was more favourable to the reagent formation in the alkaline environment. This is likely because the concentration of hydrogen ions in water decreases with the

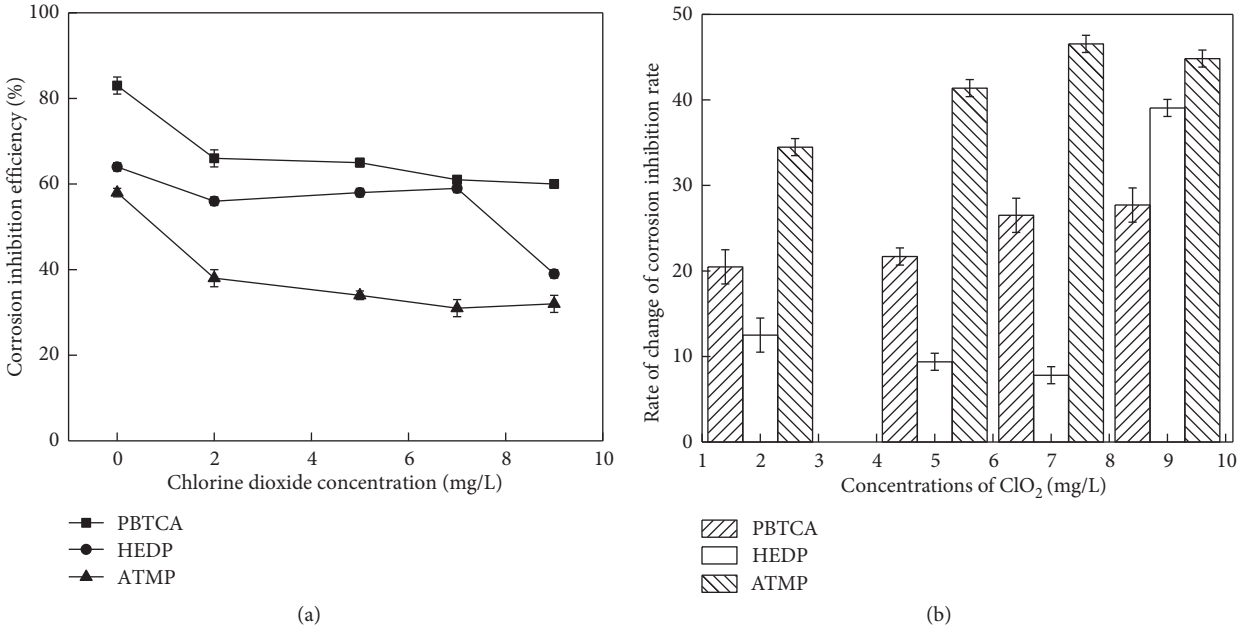

Figure 3: (a, b) Corrosion inhibition rate of carbon steels with different concentrations of ClO_2.

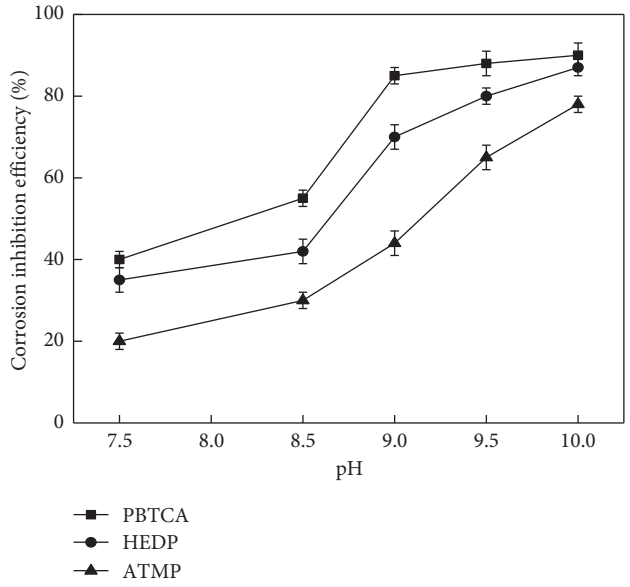

Figure 4: Corrosion inhibition rate of the corrosion inhibitor to carbon steel at different pH.

increasing pH, and thus, the depolarization of hydrogen ions in the process of metal corrosion is inhibited at high pH. Therefore, the tendency to form a protection film on the surface of carbon steel increases, as well as the corrosion inhibition rate. As shown in Figure 4, the corrosion inhibition rate of the three organic phosphorus reagents can be presented as PBTCA > HEDP > ATMP.

The influence of three factors on the inhibition of corrosion of carbon steel was studied by adding different organic phosphorus inhibitor concentrations, ClO_2 concentrations, and pH. The corrosion inhibition rate of the three organic phosphorus inhibitors was above 80%, and the average corrosion inhibition effect was satisfactory. The order of corrosion inhibition effect was PBTCA > HEDP > ATMP. In addition, with the increase in the number of P atoms, the inhibition effect of the corrosion inhibitor decreased; i.e., the corrosion inhibitor with a single phosphorus could exhibit a more effective corrosion inhibition effect.

3.2. Quantum Chemical Calculation. In order to investigate the corrosion inhibition mechanism of organic phosphorus corrosion inhibitors on carbon steel at the microscopic level, we used the density functional theory in quantum chemistry to quantify the molecular structure of organic phosphorus corrosion inhibitors, Fe, Fe^{2+}, and Zn^{2+}. Figure 1 and Table 2 show the geometric structure models and the optimized Mulliken atomic charge distributions of the three organic phosphorus inhibitors by the B3LYP/6-31G (d, p) method. As can be seen from Table 2, the P atoms were positively charged, indicating that they could accept electrons and form chemical bonds, while both N and O have a high negative charge, indicating that they could also be adsorbed onto the surface of the metal atom by the loss of electron interaction. In addition, all the C atoms in the PBTCA molecule that bonded to the C=O double bond were positively charged, while the other alkyl carbon atoms were all negatively charged; alkyl carbon and oxygen atoms in HEDP were also negatively charged; the alkyl carbon atoms in the ATMP were also negatively charged, and all the H atoms were positively charged. All these data are consistent with the results of the induced effect.

Figure 5 shows the frontier orbital diagram of the three organic phosphorus inhibitor molecules after optimization. The HOMO orbitals of the PBTCA were essentially distributed on alkyl chains and carboxyl groups linked to the

Table 2: The charge distribution of the Mulliken atom in the three corrosion inhibitors.

PBTCA		HEDP		ATMP	
Atom	Mulliken charge	Atom	Mulliken charge	Atom	Mulliken charge
P1	1.1658	P1	1.1134	C1	−0.2667
C2	−0.2905	O2	−0.5764	N2	−0.4657
C3	−0.1777	O3	−0.5953	P3	1.1046
C4	−0.2663	C4	−0.1195	C4	−0.2575
C5	−0.2588	O5	−0.6431	C5	−0.2861
O6	−0.5877	P6	1.1237	O6	−0.6589
O7	−0.5932	O7	−0.5694	O7	−0.6391
O8	−0.6405	O8	−0.6027	O8	−0.6129
C9	0.6524	O9	−0.6360	O9	−0.6436
O10	−0.5367	O10	−0.5683	O10	−0.6735
O11	−0.4980	C11	−0.3356	P11	1.1320
C12	0.6226	H12	0.3999	O12	−0.6159
O13	−0.5344	H13	0.3958	O13	−0.5825
O14	−0.5040	H14	0.4016	P14	1.1323
C15	0.5876	H15	0.4087	O15	−0.6002
O16	−0.5478	H16	0.3616	O16	−0.5800
O17	−0.4948	H17	0.1451	H17	0.1858
H18	0.1462	H18	0.1447	H18	0.1650
H19	0.1433	H19	0.1517	H19	0.1936
H20	0.1970			H20	0.1751
H21	0.1839			H21	0.1911
H22	0.1469			H22	0.1927
H23	0.1654			H23	0.4111
H24	0.3972			H24	0.3915
H25	0.4024			H25	0.4062
H26	0.3761			H26	0.3995
H27	0.3741			H27	0.4033
H28	0.3690			H28	0.3987

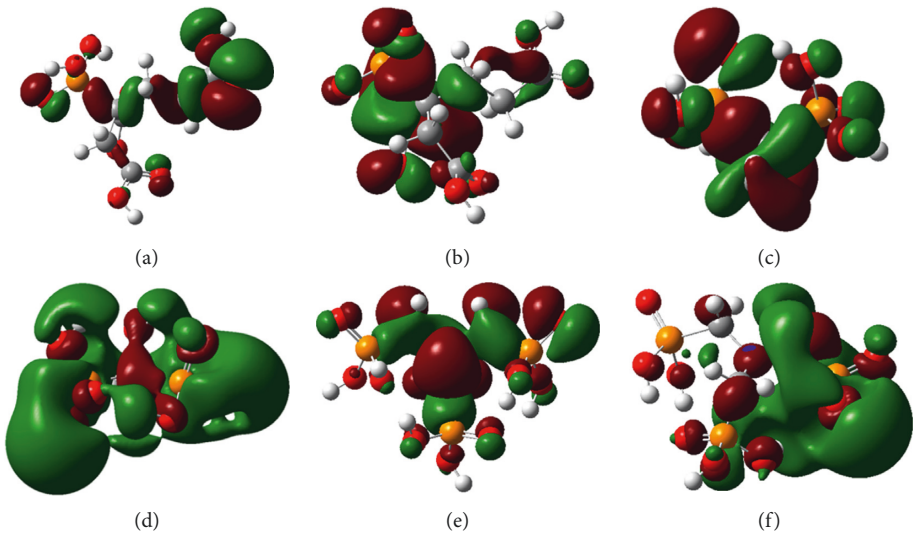

Figure 5: Optimized frontier orbitals of organic phosphorus inhibitors. (a) HOMO of PBTCA. (b) LUMO of PBTCA. (c) HOMO of HEDP. (d) LUMO of HEDP. (e) HOMO of ATMP. (f) LUMO of ATMP.

central carbon atom, while some of them were distributed near the phosphorus-oxygen double bonds belonging to the electron loss region. The LUMO orbitals were distributed near P atoms and positively charged carbon atoms which are an easy-to-accept electron region. The HOMO orbits of HEDP were located near oxygen and carbon atoms, while the LUMO orbits were located near P atoms. The HOMO orbitals of ATMP were mainly distributed near the central nitrogen and oxygen atoms, even though the LUMO orbitals were mainly distributed near the P11 atomic group.

Table 3 shows a list of quantum chemical parameters optimized for the three organic phosphorus inhibitors. The

Table 3: Quantum chemical parameters of the three organic phosphorus inhibitors at the B3LYP/6-31G (d, p) theoretical level.

Quantum chemical parameters	Corrosion inhibitor		
	PBTCA	HEDP	ATMP
E_{HOMO} (eV)	−7.5811	−7.5321	−6.4845
E_{LUMO} (eV)	−0.3320	0.6857	0.9960
ΔE (eV)	−7.2491	−8.2178	−7.4805
Dipole moment (debye)	3.7949	5.7964	12.0357
Electron affinity (A)	0.3320	−0.6857	−0.9960
Electronegativity (χ)	3.9566	3.4232	2.7443
Hardness (η)	3.6246	4.1089	3.7403
Affinity index (ω)	2.1595	1.4260	1.0068

size of E_{HOMO} represents the ability of molecules to provide electrons, while the size of E_{LUMO} represents the electron-accepting capability, and the energy gap, ΔE, represents the stability of the molecule. The smaller the value of ΔE, the more efficient the inhibitor molecule's corrosion inhibition performance. The electron-donating capacity order of the three organic phosphorus inhibitors was HEDP > PBTCA > ATMP, the electron-accepting capacity order was PBTCA > HEDP > ATMP, while the energy gap order was PBTCA < ATMP < HEDP. This reflects the high eletrophilicity of PBTCA and high nucleophilicity of ATMP. According to the three principles of orbital bonding (the orbital symmetric principle, the energy approximation principle, and the maximum overlap principle), the HOMO energies of all three corrosion inhibitors are lower than the minimum orbital energy of iron ions (0.6912 eV), which disagrees with the orbital symmetric principle. Therefore, the corrosion inhibitor molecules cannot provide electrons to empty orbits of iron atoms. The HOMO energies of all three corrosion inhibitor molecules were lower than the minimum empty orbital energy of Fe^{2+} (−1.9048 eV), which conforms to the orbital symmetric principle. Thus, HOMO energies can provide electrons to empty orbits of Fe^{2+}. The difference between HOMO orbital energy of HEDP and LUMO orbital energy of Fe^{2+} is the highest (6.1013 eV), followed by those of PBTCA (5.5092 eV) and ATMP (4.9903 eV). According to the principle of energy similarity, ATMP shows the strongest bonding capacity with Fe^{2+}, followed by PBTCA and HEDP. On the contrary, the LUMO energies of HEDP, PBTCA, and HEDP are all higher than the maximum orbital energy of iron ions (−3.0749 eV). According to the orbital symmetric principle, iron ions cannot provide electrons to HEDP and ATMP, but they can offer electrons to PBTCA. The difference between LUMO energy of PBTCA and HOMO energy of iron ions is 2.1005 eV. Although the LUMO orbital energy of the three corrosion inhibitors is higher than HOMO orbital energy of Fe^{2+}, electrons are provided to PBTCA and ATMP but not to HEDP. The differences between the LUMO orbital energies of PBTCA and ATMP and the HOMO orbital energy of Fe^{2+} are 9.1877 eV and 8.2258 eV, respectively. All three corrosion inhibitors can provide electrons to Fe^{2+} according to the comparison of the differences in HOMO orbital energy of inhibitors and LUMO orbital energy of Fe^{2+}. In conclusion, the PBTCA is superior to the other two inhibitors in terms of slow-release performance, which is similar to previous experimental results. Specifically, PBTCA can provide electrons to Fe^{2+} and receive electrons from iron atoms and can form chemical bonds with the corrosion medium in cyclic cooling water, thus avoiding corrosion.

Zn^{2+} has been proved to be an effective index of the corrosion effect in cyclic cooling water [28]. It is necessary to add corrosion inhibitors to water to inhibit corrosion upon the increase of Zn^{2+} concentration. Moreover, the composite corrosion inhibitor formed by PBTCA, HEDP, and ClO_2 presents good corrosion-relieving performance [15]. Table 3 shows that all three inhibitors can provide electrons to Zn^{2+} according to the orbital symmetric principle although their HOMO energies are lower than the LUMO energy of Zn^{2+}. The difference between the HOMO orbital energy of HEDP and the LUMO orbital energy of Zn^{2+} (−2.2177 eV) is 5.7884 eV, which is the highest relative to that of PBTCA (5.1963 eV) and that of ATMP (4.6774 eV). According to the energy similarity principle, the descending order of the three inhibitors with respect to the bonding capacity with Zn^{2+} is ATMP > PBTCA > HEDP. With abundant negative loads, oxygen atoms and nitrogen atoms in molecules of all three inhibitors easily contribute surplus electrons (Table 2). As a result, water can receive surplus electrons from the three inhibitors, which is attributed to the small content of Zn^{2+} in the water. Consequently, chemical bonds are formed and attached on the iron surface, thus further relieving the corrosion of iron. As electron buffers, all three organic phosphorus inhibitors receive electrons from iron atoms due to the positively charged phosphorus atoms. Since oxygen atoms and nitrogen atoms are rich in negative charges and provide electrons to Zn^{2+} in water, a two-layer complex is formed in the cyclic cooling water and attaches on the iron surface to protect carbon steel from corrosion. The flow graph of electrons is shown in Figure 6.

The dipole moment was caused by the uneven distribution of the atomic charges in the molecule and can, therefore, be used to measure the polarity of the inhibitor molecules. The greater the value of the dipole moment, the stronger the polarities of the molecules and the more likely the electrons are to be lost, clearly indicating the weak electron absorption between the corrosion inhibitor molecules and the metal surface. From Table 3, it can be concluded that the order of dipole moment of the three organic phosphorus molecules was ATMP > HEDP > PBTCA. The corrosion inhibitor ATMP had a better electron-donating capability. Hence, PBTCA had a better electron-receiving capability. Because of the high number of P atoms in ATMP, the steric effect was great, which was not conducive to the formation of the dense membrane. Therefore, PBTCA showed better corrosion inhibition performance.

According to Koopmans' theorem, quantum chemical parameters are related to the frontier orbital energy, such as ionization potential (I), electron affinity (A), electronegativity (χ), hardness (η), and affinity index (ω). The results are shown in Table 3.

The electron affinity potential indicates the electronic trend of the molecules, and the higher its value, the easier it is to obtain the electron. The order of electron affinity of the

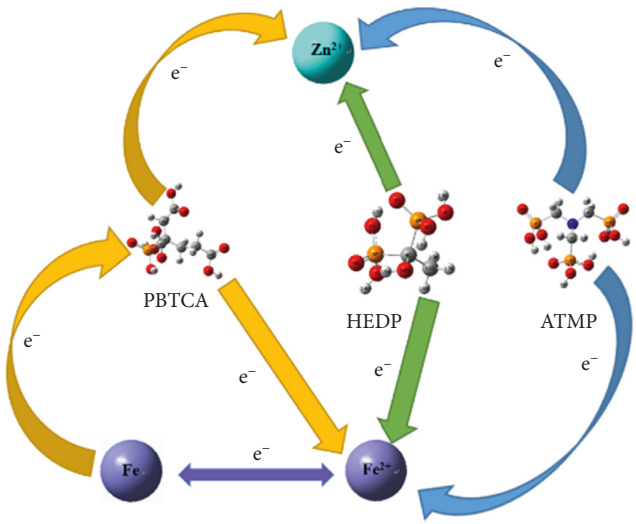

Figure 6: Electron-flow diagram of the corrosion inhibition mechanism between the inhibitor and carbon steel.

three organic phosphorus molecules was PBTCA > HEDP > ATMP. PBTCA molecules can easily obtain electrons. Electronegativity represents the ability of molecules to attract electrons. The electronegativity of the three organic phosphorus molecules was PBTCA > HEDP> ATMP, where PBTCA can easily accept electrons and react with metal atoms. Hardness can reflect stability and reactivity of molecules. The hardness of the three organic phosphorus molecules is in the order HEDP > ATMP > PBTCA. According to the principle of "hard close to hard and soft close to soft," HEDP can easily form stable products with ions. The affinity index also represents the affinity of the molecule, and the greater that value, the easier it is to attract the electrons. The three organic phosphorus corrosion inhibitors' affinity index was ranked as PBTCA > HEDP > ATMP. This clearly shows that PBTCA could accept the electrons easily, which was the main component of the three organic phosphorus corrosion inhibitors. The analysis of electron affinity, electronegativity, hardness, and electron-affinity index of the three organic phosphorus molecules also shows that PBTCA had a better corrosion inhibition performance and it was more likely to accept the free electrons outside the iron atoms and form coordination bonds. The smaller the number of P atoms contained in the molecule, the lesser its steric effect. As a result, PBTCA formed a dense protective film on the surface of the metal, thus hindering corrosion, which satisfies the requirements of prefilm in circulating cooling water.

3.3. Study on Corrosion Inhibitor Adsorption Behaviour. The adsorption isotherm of a corrosion inhibitor can describe the adsorption behaviour at a certain temperature. In order to study the adsorption models of three organic phosphorus inhibitors, we assumed that they were adsorbed on a single molecular layer on the surface of carbon steel, such that corrosion rate y was approximated by a metal surface coverage θ.

By the Langmuir adsorption isotherm, the equation is as follows:

$$\frac{\theta}{1-\theta} = KC_i. \tag{4}$$

The formula can be concluded as follows:

$$\frac{C}{\theta} = C + \frac{1}{K}, \tag{5}$$

where C is the concentration of the inhibitor (mg/L) and K is the adsorption equilibrium constant [29]. The result is shown in Figure 7.

It can be seen from Figure 7 that the regression coefficients of the organic phosphorus inhibitors were $R_{\mathrm{PBTCA}}^2 = 0.9931$, $R_{\mathrm{HEDP}}^2 = 0.9927$, and $R_{\mathrm{ATMP}}^2 = 0.9825$, respectively, indicating that the inhibitors were Langmuir adsorbed on the surface of carbon steel. The adsorption equilibrium constants were calculated using intercepts as $K_{\mathrm{PBTCA}} = 0.0732$ L/mg, $K_{\mathrm{HEDP}} = 0.0737$ L/mg, and $K_{\mathrm{ATMP}} = 0.1164$ L/mg. According to the adsorption theory, the relationship between the standard molar adsorption free energy and the adsorption equilibrium constant K is

$$K = \frac{1}{C_{\mathrm{solvent}}} \exp \frac{-\Delta G^{\theta}}{RT}, \tag{6}$$

where $C_{\mathrm{solvent}} = 55.5$, T stands for thermodynamic temperature (K), and R is the gas constant (8.314 J/mol·K). The higher the absolute value of the standard molar adsorption free energy, the higher the stability of the adsorption layer. ΔG^{θ} is negative throughout the calculation, which means that the adsorption was spontaneous. When the absolute value of ΔG^{θ} was below 20 kJ/mol, the adsorption of the inhibitor molecules on the metal surface was physical adsorption. At an absolute value of ΔG^{θ} greater than 40 kJ/mol, the corrosion inhibitor molecule formed a covalent bond with the metal surface, which shows the chemical adsorption [18]. The standard molar adsorption free energy of the three organic phosphorus molecules was obtained by introducing the adsorption equilibrium constant conversion unit into the formula, and the results were $\Delta G_{\mathrm{PBTCA}}^{\theta} = 43.414$ kJ/mol, $\Delta G_{\mathrm{HEDP}}^{\theta} = 42.743$ kJ/mol, and $\Delta G_{\mathrm{ATMP}}^{\theta} = 43.667$ kJ/mol, respectively. All values were greater than 40 kJ/mol, demonstrating that the three organic phosphorus corrosion inhibitors formed coordination bonds with the metal surface by chemical adsorption, which impedes metal corrosion.

4. Conclusion

In this paper, three organophosphorus inhibitors, PBTCA, HEDP, and ATMP, were used as the research objects, and the influence factors of corrosion inhibition efficiency and corrosion inhibition mechanism on carbon steel in circulating cooling water were discussed. The following conclusions can be drawn:

(1) The weight loss method proved that the average inhibition rate of the three organic phosphorus corrosion inhibitors was more than 80%, the inhibition rate increases with the increasing concentration of

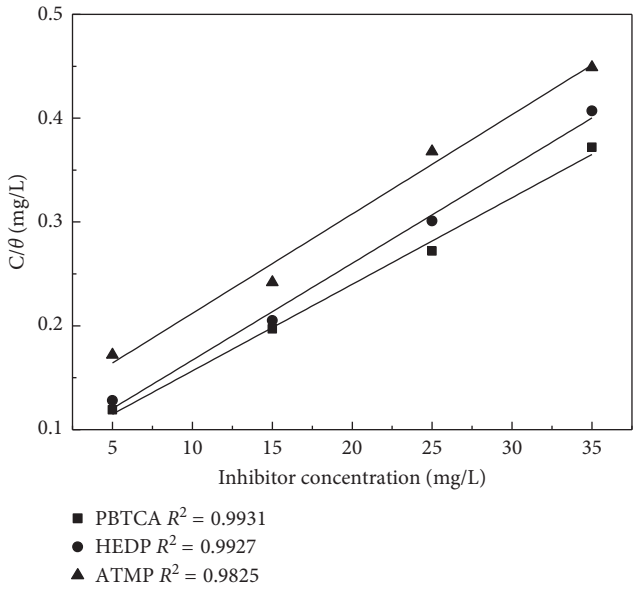

Figure 7: Isotherm fitting of three organic phosphorus inhibitors to Langmuir adsorption.

inhibitors and decreases with the increase in the number of P atoms, and the corrosion inhibition effect of single-phosphorus inhibitor PBTCA was better.

(2) The adsorption of the organophosphorus inhibitor onto the metal surface followed the Langmuir monolayer adsorption.

(3) The DFT algorithm in Gaussian 09 software was used to optimize the inhibitors at the theoretical level by the B3LYP/6-31G (d, p) method. According to molecular layout analysis and frontier orbital theory, the three organophosphorus corrosion inhibitors were used as electron buffers. By receiving the free electron of the outer orbit of the iron atom, the inhibitor and iron atom can form the stable coordination bond and form a protective film on the metal surface to obstruct the metal corrosion. At the same time, the inhibitor can provide electrons to zinc ions present in the water, forming complex compounds and meeting the requirements of the premembrane in circulating cooling water.

Data Availability

We state that the dataset(s), code, and other digital research materials supporting the results in the article are available from the corresponding author upon request.

Ethical Approval

Research ethics: we state that we did not receive ethical approval from a local ethics committee to carry out our study. Animal ethics: we state that we did not obtain the necessary licences and approvals from our institutional animal ethics committee before conducting our research.

Conflicts of Interest

The authors declare that they have no conflicts of interest.

Acknowledgments

We would like to thank Harbin Gas Works for making available the corrosion agents for the study. Furthermore, we wish to thank the Harbin Institute of Technology. Liu Liang is grateful for a funded PhD stipend provided by the Nanqi Ren Studio. The research was supported by the Nanqi Ren Studio, Academy of Environment and Ecology, Harbin Institute of Technology (grant number HSCJ201704).

References

[1] T. F. Tang, "Optimization of compound scale corrosion inhibitor formula for circulating cooling water," *Environmental Science and Technology*, vol. 27, pp. 126–128, 2004.

[2] C. F. Wei, L. Hong, and B. F. Liang, "Status and development of corrosion and scaleinhibitors for circulating cooling water," *Science and Technology of lcic*, vol. 5, pp. 126–128, 2000.

[3] D. M. Wei, "Treatment of circulating cooling water in Refrigeration system," *Technology and Development of Chemical Industry*, vol. 1, pp. 42–57, 2011.

[4] R. Touir, N. Dkhireche, M. Ebn Touhami et al., "Study of phosphonate addition and hydrodynamic conditions on ordinary steel corrosion inhibition in simulated cooling water," *Materials Chemistry and Physics*, vol. 122, no. 1, pp. 1–9, 2010.

[5] Z. Quan, C. Wang, B. Li, Y. Chen, and C. Ma, "Experimental study of circulating cooling water scale inhibition by low voltage electrostatic," *Water Purification Technology*, vol. 6, pp. 1–9, 2007.

[6] F. Tang, A. P. Zheng, and Z. Z. Song, "Research progress and application of scale inhibitors for industrial circulating cooling water," *Science and Technology in Chemical Industry*, vol. 3, pp. 1–9, 2010.

[7] Y. Wang, "Mechanism and control countermeasures of scale and corrosion in circulating water," *Petrochemical Technology*, vol. 7, p. 43, 2017.

[8] E. Ilhan-Sungur and A. Otuk, "Microbial corrosion of galvanized steel in a simulated recirculating cooling tower system," *Corrosion Science*, vol. 52, no. 1, pp. 161–171, 2010.

[9] F. Liu, X. Lu, W. Yang, J. Lu, and H. Zhong, "Optimizations of inhibitors compounding and applied conditions in the simulated circulating cooling water system," *Desalination*, vol. 313, pp. 18–27, 2013.

[10] R. Liang, J. Li, M. Liu, and Z. Y. Huang, "Influence of inhibitors on the adhesion of SRB to the stainless steel in circulating cooling water," *Colloids and Surfaces B: Biointerfaces.*vol. 172, pp. 1–9, 2018.

[11] K. H. Rahmani, R. Jadidian, and S. Haghtalab, "Evaluation of inhibitors and biocides on the corrosion, scaling and biofouling control of carbon steel and copper-nickel alloys in a power plant cooling water system," *Desalination*, vol. 393, pp. 1174–1185, 2016.

[12] C. Hou, "Corrosion control, fouling deposit control and biofouling control in the seawater circulating cooling system," *Ocean Technology*, vol. 4, pp. 1174–1185, 2002.

[13] K. Rahmani, "Reducing water consumption by increasing the cycles of concentration and Considerations of corrosion and scaling in a cooling system," *Applied Thermal Engineering*, vol. 114, pp. 849–856, 2017.

[14] Y. J. Teng, S. H. Shao, and C. W. Cui, "Study on compatibility of chlorine dioxide with organic phosphine reagents," *Journal of Harbin Commercial University (Natural Science Edition)*, vol. 3, pp. 313–315, 2008.

[15] X. H. He, J. W. Mao, Q. Ma, and Y. M. Tang, "Corrosion inhibition of perimidine derivatives for mild steel in acidic media: electrochemical and computational studies," *Journal of Molecular Liquids*, vol. 268, pp. 260–268, 2018.

[16] E. S. H. E. Ashry and S. A. Senior, "QSAR of lauric hydrazide and its salts as corrosion inhibitors by using the quantum chemical and topological descriptors," *Corrosion Science*, vol. 53, pp. 1025–1034, 2011.

[17] G. Gece, "The use of quantum chemical methods in corrosion inhibitor studies," *Journal of Molecular Liquids*, vol. 50, no. 11, pp. 2981–2992, 2008.

[18] H. Hamani, T. Douadi, D. Daoud, M. Ai-Noaimi, and R. A. Rikkouh, "1-(4-Nitrophenyl-imino)-1-(phenylhydrazone)-propane-2-one as a corrosion inhibitor for mild steel in 1 M HCl solution: weight loss, electrochemical, thermodynamic and quantum chemical studies," *Journal of Electroanalytical Chemistry*, vol. 801, pp. 425–438, 2017.

[19] A. A. Olajire, "Corrosion inhibition of offshore oil and gas production facilities using organic compound inhibitors - a review," *Journal of Molecular Liquids*, vol. 248, pp. 775–808, 2017.

[20] S. Kumar, D. Sharma, and P. Yadav, "Experimental and quantum chemical studies on corrosion inhibition effect of synthesized organic compounds on N80 steel in hydrochloric acid," *Industrial and Engineering Chemistry Research*, vol. 52, no. 39, pp. 14019–14029, 2013.

[21] G. Gece and S. Bilgi, "Molecular-level understanding of the inhibition efficiency of some inhibitors of zinc corrosion by quantum chemical approach," *Industria and Engineering Chemistry Research*, vol. 51, no. 43, pp. 14115–14120, 2012.

[22] X. Shi, Y. Jiang, H. Wang, Y. Hao, and S. Chen, "Density functional theory study on adsorption behavior of four pyrazine inhibitors on Cu (111) surface," *Journal of Chemical Engineering*, vol. 68, pp. 3211–3217, 2017.

[23] C. W. Cui, S. F. Li, H. Yang, W. T. Feng, and Y. Liu, "Theoretical study of corrosion inhibition of PBTCA, HEDP, ATMP," *Material Science and Technology*, vol. 14, pp. 608–611, 2006.

[24] Y. M. Chen, C. X. Sun, Y. S. Cheng, M. Zhang, and M. Chen, "Study on corrosion inhibition of carbon steel, copper and stainless steel by the polyaspartic acid compound," *Application of Chemical Industry*, vol. 43, pp. 647–650, 2014.

[25] I. B. Obot, D. D. Macdonald, and Z. M. Gasem, "Density functional theory (DFT) as a powerful tool for designing new organic corrosion inhibitors. Part 1: an overview," *Corrosion Science*, vol. 99, pp. 1–30, 2015.

[26] P. Geerlings, F. De Proft, and W. Langenaeker, "Conceptual density functional theory," *Chemical Reviews*, vol. 103, no. 5, pp. 1793–1873, 2003.

[27] D. B. Hmamou, R. Salghi, A. Zarrouk, M. R. Aouad, and O. Benali, "Weight loss, electrochemical, quantum chemical calculation, and molecular dynamics simulation studies on 2-(Benzylthio)-1,4,5-triphenyl-1H-imidazole as an inhibitor for carbon steel corrosion in hydrochloric acid," *Industrial and Engineering Chemistry Research*, vol. 52, no. 40, pp. 14315–14327, 2013.

[28] L. Liu, T. T. Cao, Q. W. Zhang, and C. W. Cui, "Optimization of associative model between chlorine dioxide and organo-phosphorus corrosion inhibitor by RSM-BBD," *Industrial Water Treatment*, vol. 12, 2018.

[29] H. Gerengi, M. Mielniczek, G. Gece, and M. M. Solomon, "Experimental and quantum chemical evaluation of 8-hydroxyquinoline as a corrosion inhibitor for copper in 0.1 M HCl," *Industrial and Engineering Chemistry Research*, vol. 55, no. 36, pp. 9614–9624, 2016.